IVYSPRING INTERNATIONAL PUBLISHER

Theranostics

2018; 8(8): 2161-2170. doi: 10.7150/thno.23335

Research Paper

Tumor-targeted Dual-modality Imaging to Improve Intraoperative Visualization of Clear Cell Renal Cell Carcinoma: A First in Man Study

Marlène C. Hekman[1,2]✉, Mark Rijpkema[1], Constantijn H. Muselaers[2], Egbert Oosterwijk[2], Christina A. Hulsbergen-Van de Kaa[3], Otto C. Boerman[1], Wim J. Oyen[1,4], Johan F. Langenhuijsen[2], Peter F. Mulders[2]

1. Department of Radiology and Nuclear Medicine, Radboudumc, Nijmegen, The Netherlands.
2. Department of Urology, Radboudumc, Nijmegen, The Netherlands.
3. Department of Pathology, Radboudumc, Nijmegen, The Netherlands.
4. The Institute of Cancer Research and The Royal Marsden Hospital, London, United Kingdom.

✉ Corresponding author: Marlène C.H. Hekman, Dept. of Radiology & Nuclear Medicine, Geert Grooteplein-Zuid 10, 6525 GA, Nijmegen, marlene.hekman@radboudumc.nl, Tel: 024-3614048, Fax: 024- 3618942.

Received: 2017.10.15; Accepted: 2018.02.09; Published: 2018.03.08

Abstract

Intraoperative imaging with antibodies labeled with both a radionuclide for initial guidance and a near-infrared dye for adequate tumor delineation may overcome the main limitation of fluorescence imaging: the limited penetration depth of light in biological tissue. In this study, we demonstrate the feasibility and safety of intraoperative dual-modality imaging with the carbonic anhydrase IX (CAIX)-targeting antibody ^{111}In-DOTA-girentuximab-IRDye800CW in clear cell renal cell carcinoma (ccRCC) patients.

Methods: A phase I protein dose escalation study was performed in patients with a primary renal mass who were scheduled for surgery. ^{111}In-DOTA-girentuximab-IRDye800CW (5, 10, 30, or 50 mg, n=3 ccRCC patients per dose level) was administered intravenously and after 4 days SPECT/CT imaging was performed. Seven days after antibody injection, surgery was performed with the use of a gamma probe and near-infrared fluorescence camera.

Results: In total, fifteen patients were included (12 ccRCC, 3 CAIX-negative tumors). No study-related serious adverse events were observed. All ccRCC were visualized by SPECT/CT and localized by intraoperative gamma probe detection (mean tumor-to-normal kidney (T:N) ratio 2.5 ± 0.8), while the T:N ratio was 1.0 ± 0.1 in CAIX-negative tumors. ccRCC were hyperfluorescent at all protein doses and fluorescence imaging could be used for intraoperative tumor delineation, assessment of the surgical cavity and detection of (positive) surgical margins. The radiosignal was crucial for tumor localization in case of overlying fat tissue.

Conclusion: This first in man study shows that tumor-targeted dual-modality imaging using ^{111}In-DOTA-girentuximab-IRDye800CW is safe and can be used for intraoperative guidance of ccRCC resection.

Key words: carbonic anhydrase IX, clear cell renal cell carcinoma, intraoperative dual-modality imaging, fluorescence imaging, image-guided surgery

Introduction

Intraoperative fluorescence imaging has proven to be valuable in cancer surgery to enhance tumor visualization in challenging situations such as multifocal disease [1] or organ-sparing surgery [2]. It can be used to differentiate tumor from normal tissue. By conjugating a fluorescent dye to a monoclonal

antibody against a tumor-specific antigen, a tumor-targeting fluorescent tracer can be created. Several studies have already shown the feasibility of this tumor-targeted approach for intraoperative fluorescence imaging [3-5]. However, the major pitfall of fluorescence imaging is the limited penetration depth of light in tissue, restricting detection to superficial tumors. This inherent problem can be overcome by combining fluorescence imaging with radiodetection, as gamma radiation has a high penetration depth in tissue. By dual-labeling monoclonal antibodies with a radionuclide for initial guidance and a near-infrared dye for real-time tumor delineation, the advantages of radiodetection and fluorescence imaging are combined. Due to specific accumulation of the antibody in tumor tissue, tumor-targeted dual-modality imaging may guide the surgeon to perform a complete tumor resection. We now describe the first in man study using this tumor-targeted dual-modality imaging technique during surgery.

Approximately 115,000 patients are diagnosed with renal cell carcinoma (RCC) in Europe every year [6]. A large proportion of these patients is treated by nephron-sparing surgery (NSS) with a trend towards NSS of larger or more complex tumors [7, 8]. Positive surgical margins (PSM) after NSS are seen in up to 7% of patients, but percentages up to 15% are reported in NSS for imperative indications (e.g., solitary kidney) [9]. Improved intraoperative tumor visualization by dual-modality imaging may help to perform oncologically safe NSS. Girentuximab is a monoclonal antibody that recognizes carbonic anhydrase IX (CAIX) that has been used extensively to target clear cell RCC (ccRCC), since more than 95% of ccRCC express CAIX [10-13]. Preclinical studies with dual-labeled girentuximab have shown the feasibility of tumor-targeted dual-modality imaging [14-17]. Thus, this technique may be useful during surgery to localize, visualize and delineate ccRCC. Furthermore, it may be used to detect residual tumor tissue or PSM and thereby improve the outcome of surgery.

The aim of this clinical trial was to evaluate the safety of ^{111}In-DOTA-girentuximab-IRDye800CW and to demonstrate the feasibility of preoperative as well as intraoperative detection of ccRCC with this CAIX-targeted dual-modality imaging agent.

Materials and Methods

Study design

This was a single center phase I protein dose escalation study in adult patients with a primary renal mass who were scheduled for partial or radical nephrectomy. The focus of the trial design was to collect safety data and to collect data that support the intended clinical use and indication statement [18]. Written informed consent was obtained from all patients. Patients with a known non-ccRCC subtype were excluded. Because preclinical data in primates suggested that another antibody-IRDye800CW conjugate influenced corrected QT (QTc) intervals, a measurement for electrical depolarization and repolarization of the hearts' ventricles [19], patients with a pre-existent prolonged QTc interval were excluded. ^{111}In-DOTA-girentuximab-IRDye800CW (5, 10, 30, or 50 mg, n=3 ccRCC patients per dose level) was administered intravenously and after 4 days SPECT/CT imaging was performed. Seven days after antibody injection, surgery was performed with the use of a gamma probe and near-infrared fluorescence camera. The aim of this study was to demonstrate the safety and feasibility of intraoperative dual-modality imaging with the carbonic anhydrase IX (CAIX)-targeting antibody ^{111}In-DOTA-girentuximab-IRDye 800CW in clear cell renal cell carcinoma (ccRCC) patients. Safety was scored by the number of adverse events (AE) according to the common terminology criteria for adverse events version 4.0 (CTCAE v4.0). Feasibility was defined as the ability to detect a discriminatory fluorescence and/or radioactive signal in ccRCC tumor tissue compared to normal kidney tissue. Patients with a CAIX-negative tumor on final histology were only included in the safety analysis. The study was approved by the regional Medical Ethics Committee of the region Arnhem-Nijmegen and was registered on clinicaltrials.gov (NCT: 02497599). A study flowchart of the design of the study is shown in Fig. S1.

Preparation of ^{111}In-DOTA-girentuximab-IRDye800CW

DOTA-girentuximab-IRDye800CW was produced under metal free conditions and protected from light and production complied with Good Manufacturing Practice quality. Chimeric girentuximab 5 mg/mL (Wilex AG, Munich, Germany) was incubated with a 2−2.5-fold molar excess (preferred conjugation ratio 0.5-2.0) of IRDye800CW-NHS ester (LI-COR biosciences, Lincoln, NE, USA) and next with a 25-fold molar excess (preferred conjugation ratio of 0.5-3.0) of the chelator DOTA-NHS ester (Macrocyclics, Dallas, TX, USA) in a 1.25 M $NaHCO_3$ buffer pH 8.5. Excess IRDye800CW-NHS ester and DOTA-NHS ester were removed by dialysis against 0.25 M ammoniumacetate pH 5.5 for 3 days. The integrity of the dual-labeled antibody conjugate was checked before i.v. administration. Radiochemical purity after radiolabeling was determined by high-performance liquid chromatography analysis. The integrity of the antibody-dye conjugate was checked

by measuring the amount of free IRDye800CW in the preparation by high-performance liquid chromategraphy. To confirm the tumor-specific binding of the dual-labeled antibody, the immunoreactive fraction of ^{111}In-DOTA-girentuximab-IRDye800CW was determined as described by Lindmo [20] and exceeded 70%. DOTA-girentuximab-IRDye800CW was stored in the dark at 4 °C until use.

Radiolabeling was performed by incubating DOTA-girentuximab-IRDye800CW during 30 min at 45 °C with 100-120 MBq of Indium-111 (Mallinckrodt Pharmaceuticals, 's Hertogenbosch, The Netherlands). Unlabeled DOTA-girentuximab-IRDye800CW was added to obtain the required protein dose. Radiochemical purity was determined by high-performance liquid chromatography. 100 MBq of the final product was diluted in NaCl 0.9% to a final volume of 10 mL and pulled up in a syringe shortly before injection. Two patients received only 75 MBq instead of 100 MBq due to technical problems. Standards of the injected dose (ID) were prepared in triplicate to be able to quantify antibody accumulation in surgically obtained tissue samples.

Dual-labeled girentuximab injection

Seven days before surgery, patients were injected intravenously with ^{111}In-DOTA-girentuximab-IRDye800CW (100 MBq). Previous studies with radiolabeled girentuximab have shown an optimal protein dose of 5-10 mg [10, 12]. Since this was the first clinical trial with ^{111}In-DOTA-girentuximab-IRDye800CW and conjugation of IRDye800CW slightly changes the biodistribution of girentuximab [15], the dose escalation study was repeated. The rationale for the dose escalation schema was to determine the dose with the highest tumor-to-normal tissue ratio and the best intraoperative signal for both imaging modalities. Protein doses of 5, 10, 30 or 50 mg were chosen in the current study. At each protein dose level three patients were included. When final histology revealed a CAIX-negative tumor, the patient was replaced by a subsequent patient at that dose level. Patients were monitored for AE for three hours and ECG-monitoring with measurement of the QTc interval was performed before and after injection. Blood samples were taken for pharmacokinetic and safety analyses.

SPECT/CT imaging

Four days after injection whole body anterior and posterior gamma camera images and SPECT/CT imaging of the abdomen were performed with a dual-head Symbia T16 Truepoint SPECT/CT scanner (Siemens Healthcare, The Hague, The Netherlands). After acquisition of a low dose, non-contrast enhanced CT, scintigraphic imaging was performed clockwise continuously from 0-180°, with 64 views, 19 s per view with medium energy all-purpose parallel-hole collimators. Accumulation of ^{111}In-DOTA-girentuximab-IRDye800CW in tumors was scored as absent or present by an experienced nuclear medicine physician (WO).

Dual-modality image-guided surgery

Standard of care surgery was performed, supplemented with gamma probe detection and near-infrared fluorescence imaging (NIRF) to assess accumulation of ^{111}In-DOTA-girentuximab-IRDye800-CW in the tumor. Intraoperative scintillation counting was performed with the SOE 311-AL laparoscopic gamma probe with a lateral window (diameter 10 mm, length 38.7 cm) or the Europrobe 1 for open surgery (Eurorad, Strasbourg, France). An intraoperative tumor-to-normal kidney tissue ratio (T:N) was calculated by dividing the maximum counts per second (cps) in tumor by the maximum cps in adjacent ipsilateral normal kidney tissue. NIRF was performed with the Karl Storz NIR/ICG System (Karl Storz GmbH & co, Tuttlingen, Germany) for laparoscopic surgery, or the QMI Spectrum NIR fluorescence camera for both laparoscopic and open surgery (Quest Medical Imaging, Middenmeer, The Netherlands). In addition, *ex vivo* dual-modality imaging of the resected specimens was performed.

Tissue analyses

NIRF and autoradiography were performed on a tissue slice of the resected specimen as described previously [17]. In short, a 5-10 mm thick slice of the resected specimen containing tumor and normal kidney tissue was obtained from the pathology department. First, NIRF was done using the Odyssey flatbed fluorescence scanner (800 nm channel, focus 1.0 mm) (LI-COR biosciences, Lincoln, NE). Next, autoradiography was performed by exposing a phosphor imaging plate for approximately one hour to the tissue slice. This plate was developed using the Typhoon FLA 7000 Phosphor Imager and analyzed with Aida Image Analyzer v. 4.21. To quantify tissue accumulation of ^{111}In-DOTA-girentuximab-IRDye800-CW, samples of tumor and normal kidney parenchyma from the tissue slice and samples of blood were taken, weighed and measured in a gamma counter (2480 WIZARD^2, Perkin Elmer, Boston, MA) together with aliquots of the injected dose. Tracer accumulation was expressed as percentage of the injected dose per gram of tissue (%ID/g). Next, the 5-10 mm thick tissue slice was fixed in formalin and embedded in paraffin. In case of partial nephrectomy specimens, the tissue slice was embedded in its

entirety to be able to compare signal distribution in the tissue slices with the tissue sections. Fluorescence imaging of the tissue sections was done using the Odyssey flatbed fluorescence scanner (800 nm channel, focus 1.0 mm). Finally, hematoxylin and eosin staining and M75-staining for CAIX-expression were performed on 4 µm formalin-fixed paraffin-embedded tissue sections and interpreted by a uropathologist.

Statistics

Statistical analyses were performed using IBM SPSS Statistics 22.0. One-way ANOVA testing with post-hoc Bonferroni correction was performed to test for significant differences between the different protein dose levels in T:N ratios. Independent sample t-tests were performed to compare mean T:N ratios and tracer accumulation (%ID/g) between ccRCC and CAIX-negative tumors and a paired t-test to compare tracer accumulation between tumor and normal kidney tissue. Values are expressed as mean with standard deviation (SD). An alpha of 0.05 was used in all analyses and $p<0.05$ was considered significant. The biological half life of ^{111}In-DOTA-girentuximab-IRDye800CW was calculated using bi-exponential regression analysis in MATLAB version R2014b. Graphs were made using GraphPad Prism 5.03.

Results

Patient population

Written informed consent was obtained from 17 patients with a primary renal mass who were scheduled for partial or radical nephrectomy. Two of these patients were excluded before injection of ^{111}In-DOTA-girentuximab-IRDye800CW because of a prolonged QTc-interval. Three patients with a CAIX-negative tumor were replaced. An overview of patient characteristics is given in Table 1 and a study flowchart can be found in Fig. S1.

Safety analysis

All 15 patients were monitored for three hours after antibody injection and no infusion-related (serious) adverse events ((S)AE) nor any significant changes in vital signs were observed. ECG-analysis before and one hour after antibody injection showed no prolongation of the QTc interval. Blood samples that were taken for pharmacokinetic and safety analysis revealed no significant abnormalities in blood values after antibody injection. Five possibly related grade 1 AE were observed, while all other AE were related to surgery (Table S1).

Preoperative SPECT/CT imaging

All CAIX-expressing tumors were visualized preoperatively by SPECT/CT, while no uptake was seen in CAIX-negative tumors (patients #13-15). Some physiological liver uptake was observed. False positive accumulation of ^{111}In-DOTA-girentuximab-IRDye800CW was observed by SPECT/CT in a CAIX-negative adrenal adenoma and a cyst in the contralateral kidney in patient #12. In patient #6, accumulation of ^{111}In-DOTA-girentuximab-IRDye-800CW was visualized by the SPECT in a known bone metastasis (first lumbar vertebra). Unfortunately, this lesion was not accessible for intraoperative imaging during surgery (not in the surgical field). The other patients did not have metastatic disease.

Intraoperative dual-modality imaging

During surgery, all 12 ccRCC could be localized by gamma probe measurements with a mean (T:N) ratio of 2.5 ± 0.8 (Fig. 1 and Movie S1), while the T:N ratio in the 3 CAIX-negative tumors was significantly lower (1.0 ± 0.1, $p<0.05$). The highest T:N ratio (3.3 ± 0.6) was observed in the 10 mg dose group. T:N ratios did not differ significantly between the various protein doses ($p=0.22$). Radioactive probe guidance proved to be essential for intraoperative tumor localization, especially when fat covered the tissue of interest, since the fluorescence signal was significantly attenuated by the perinephric fat.

After tumor localization and exposure of the tumor, NIRF was used for real-time tumor visualization and differentiation of tumor from normal kidney tissue (Fig. 2, Fig. 3 and Movie S2). Hyperfluorescence of tumors was observed during surgery and/or on the bench in all ccRCC at all protein dose levels. Fluorescence of normal kidney parenchyma was low (Fig. 2). Fluorescence imaging during open surgery was straightforward, but for laparoscopic surgery a perpendicular approach of the tumor with the fluorescence camera proved to be essential for accurate NIRF imaging. This was a complicating factor in laparoscopic surgery, especially in posterior tumors. Iso- or hypofluorescence was observered in two out of three CAIX-negative tumors (patients #14 and #15), while hyperfluorescence was observed in one CAIX-negative pseudocystic lesion (patient #13), but since no radioactive signal was detectable, it was considered to be autofluorescence of the cyst content.

One PSM was correctly identified by ex vivo NIRF of the resected specimens (patient #11). Additionally, resected tissue contained vital tumor, as confirmed by histopathology (Fig. 3). In all other ccRCC, a rim of hypofluorescent, normal kidney parenchyma was visible around the tumor and final histology confirmed negative surgical margins.

Table 1. Patients characteristics.

No. #	Dose (mg)	Age	Sex	Tumor size (cm)	Surgery	T-stage	Pathological margin	Histology	CAIX
1	5	67	F	6.0	RALN	pT1b	R0	ccRCC	+
2	5	71	F	3.6	RALPN	pT1a	R0	ccRCC	+
3	5	76	F	8.0	LN	pT1b	R0	ccRCC	+
4	10	59	M	3.3	RALPN	pT1a	R0	ccRCC	+
5	10	75	M	5.0	LN	pT1b	R0	ccRCC	+
6	10	76	M	6.0	LN	pT1b (M1)	R0	ccRCC	+
7	30	69	M	2.5	RALPN	pT1a	R0	Papillary ccRCC	+
8#	30	76	M	2.5	RALPN	pT1a	R0	ccRCC	+
9	30	55	F	2.8	OPN	pT1a	R0	ccRCC	+
10	50	58	M	5.7	RALPN	pT1b	R0	ccRCC	+
11	50	57	F	5.4	OPN	pT3a	R1*	ccRCC	+
12	50	65	M	3.7	RALPN	pT1a	R0	ccRCC	+
13	30	64	M	1.5	RALPN	-	R0	Pseudocyst	-
14	50	63	M	3.2 & 1.8	RALPN	-	R1	Angiomyolipomas	-
15	50	76	V	2.5	RALPN	pT1a	R0	Clear cell papillary RCC	-

LN: laparoscopic nephrectomy; OPN: open partial nephrectomy; RAL(P)N: robot-assisted laparoscopic (partial) nephrectomy.

#Due to logistical reasons, surgery in patient 8 was performed 6 days after injection (instead of 7).

*Tumor tissue was present in the deep surgical margin of the primary resected specimen and further resection contained vital tumor tissue. Since the tumor was not resected *en bloc*, unequivocal assessment of the surgical margin was not possible.

Tissue analyses

A high T:N fluorescence contrast was seen in all ccRCC by fluorescence imaging of the 5-10 mm slices of the resected specimens (Fig. S2). Considerable intratumoral heterogeneity in the uptake of ^{111}In-DOTA-girentuximab-IRDye800CW was observed macroscopically, with high uptake at the tumor borders and lower uptake in the tumor center, most likely due to perfusion differences limiting tumoral penetration of girentuximab. Histopathology of the tissue section showed homogeneous expression of CAIX in tumors coinciding with the distribution of the fluorescence signal (Fig. 4).

Maximum tumor uptake of ^{111}In-DOTA-girentuximab-IRDye800CW in ccRCC as measured with a gamma counter ranged from 0.04–0.58 %ID/g, while uptake was significantly lower in normal kidney tissue (mean 0.004±0.002 %ID/g, $p<0.05$). In CAIX-negative tumors, 0.01±0.01 %ID/g ^{111}In-DOTA-girentuximab-IRDye800CW was detected, possibly related to the enhanced permeability and retention effect.

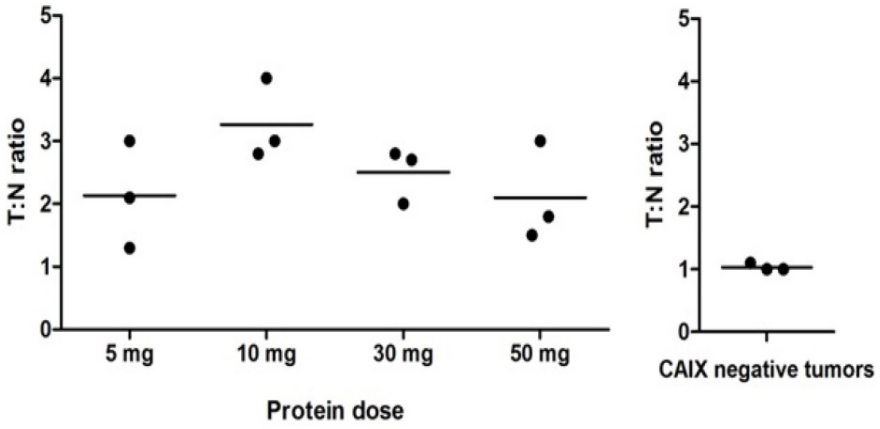

Figure 1. Intraoperative gamma probe measurements (T:N ratios). Each dot represents one patient and the horizontal line represents the mean per dose level. The highest T:N ratios were observed after administration of 10 mg ^{111}In-DOTA-girentuximab-IRDye800CW, but differences between the dose levels were not statistically significant. The T:N ratio in the CAIX-negative tumors was significantly lower than in the CAIX-positive tumors ($p<0.05$).

Pharmacokinetic analyses

The average blood levels of ^{111}In-DOTA-girentuximab-IRDye800CW were 0.024±0.009, 0.019±0.007, 0.007±0.003 and 0.004±0.002 %ID/g at 5 min, 3 h, 4 d and 7 d post injection, respectively. When fitting the curves in a two-compartment model, the half life in the distribution phase was 1.4±1.7 h ($t_{1/2}\alpha$) and in the clearance phase 73.5±17.0 h ($t_{1/2}\beta$) (Fig. 5).

Discussion

This study describes the first clinical application of tumor-targeted dual-modality imaging with a dual-labeled monoclonal antibody. It shows that this novel technique is safe and allows successful intraoperative visualization of tumors in patients with ccRCC. Combining a radiolabel for preoperative imaging and intraoperative probe-guided tumor localization and a fluorescent label for tumor delineation proved to be a powerful synergy. CcRCC could be localized intraoperatively by gamma probe detection, and after surgical exposure of the tumor, NIRF could be used to delineate tumors and detect PSM. This potential of targeted dual-modality imaging can also be exploited in many other cancer types, by replacing girentuximab by another tumor-targeting antibody.

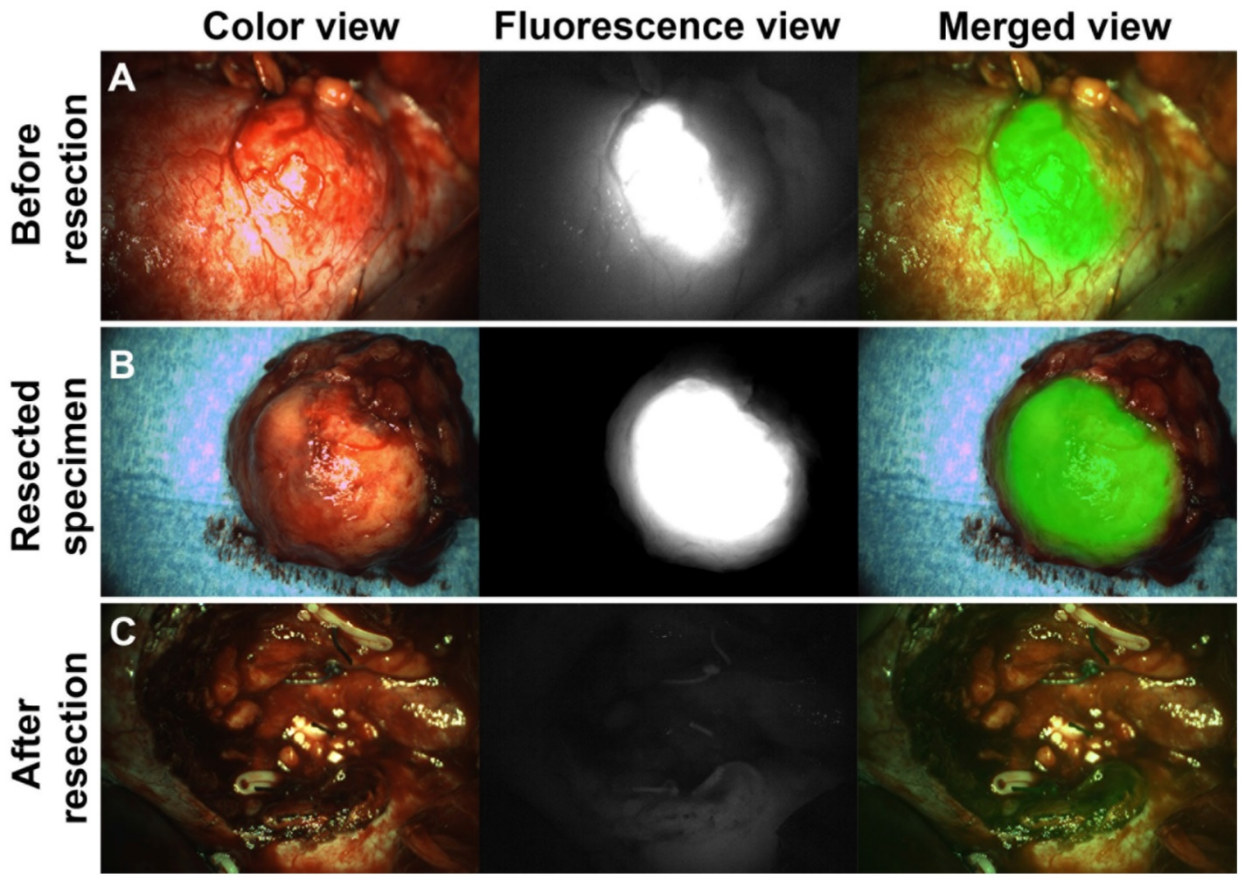

Figure 2. Intraoperative NIRF to guide complete tumor resection (patient #9). **(A)** Intraoperative NIRF before tumor resection: Hyperfluorescence of a ccRCC was seen after injection of ^{111}In-DOTA-girentuximab-IRDye800CW. NIRF was successfully used for tumor border delineation. **(B)** *Ex vivo* NIRF of the resected specimen showed a rim of normal hypofluorescent tissue around the hyperfluorescent tumor indicating a negative surgical margin, as confirmed by histopathology. **(C)** Intraoperative NIRF of the surgical cavity after tumor resection indicated complete tumor removal.

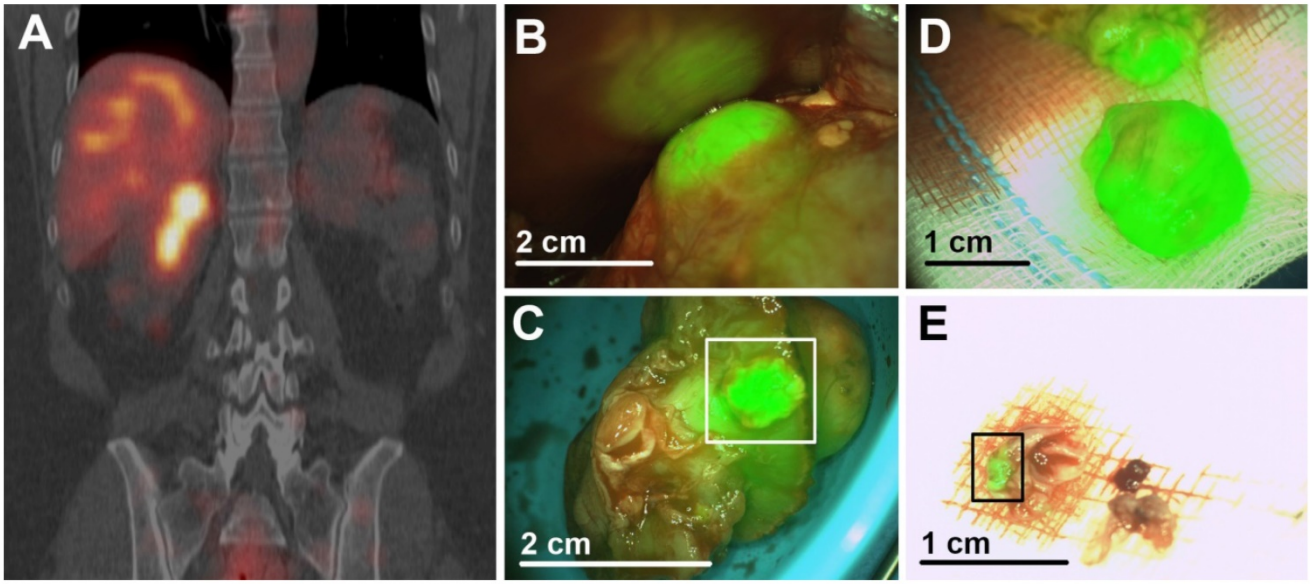

Figure 3. Dual-modality imaging after injection of ^{111}In-DOTA-girentuximab-IRDye800CW (patient #11). **(A)** Preoperative SPECT/CT imaging confirmed the presence of a CAIX-expressing ccRCC and revealed that this tumor extended deep into this patients' monokidney. **(B)** Intraoperative NIRF showed hyperfluorescence of the tumor. **(C)** Assessment of the resected tumor specimen with NIRF suggested tumor in the surgical margin (square), which was subsequently confirmed by histopathology. **(D)** NIRF demonstrated that further resection contained vital tumor, again confirmed by histopathology. **(E)** NIRF was used to assess the presence of tumor (square) in additional resected tissue fragments. Histopathology confirmed that the fragment consisted mainly of fibrotic tissue, but also a tumor fragment of 2 mm. Scale bars are an approximation.

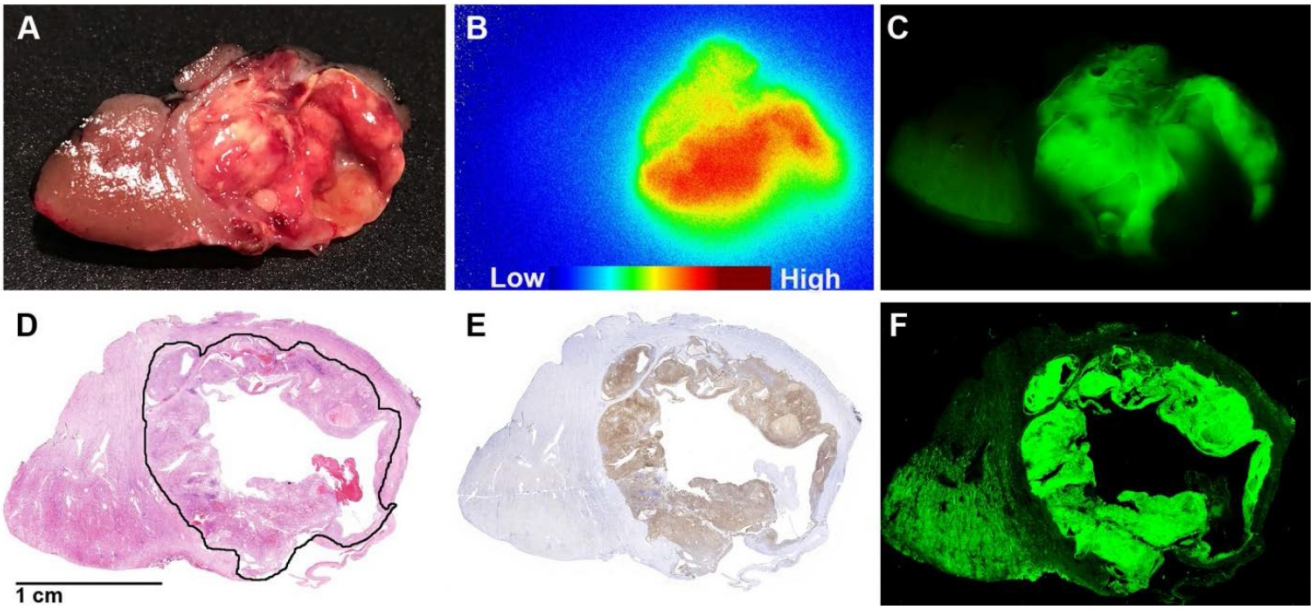

Figure 4. Tissue processing and tissue section analysis (patient #8). Thin (5-10 mm) tissue slices **(A)** of the resected specimens were analyzed by autoradiography **(B)** and near-infrared fluorescence imaging **(C)**. Both the radioactive and fluorescence signals were localized in tumor tissue. Histopathology of a tissue section showed homogeneous expression of CAIX in tumors coinciding with the distribution of the fluorescence signal. **(D)** H&E staining with the tumor annotated. **(E)** M75-staining showed a high and homogenous expression of CAIX in the tumor, visually overlapping with the distribution of the fluorescence signal. **(F)** Fluorescence imaging of a tissue section showed that T:N contrast is high at the tumor borders.

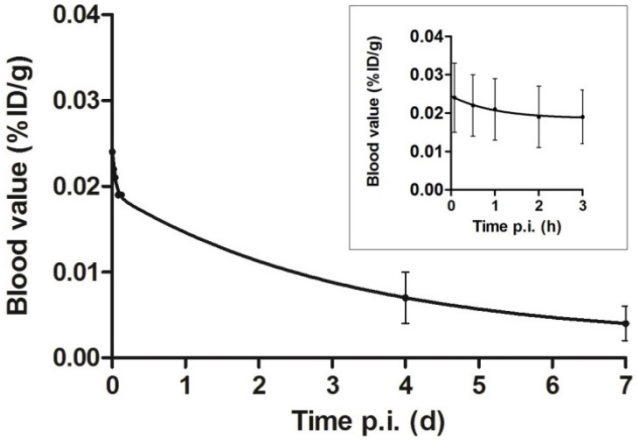

Figure 5. Blood clearance of dual-labeled girentuximab over seven days after injection (p.i.) fitted to a two-compartment model. Inset: clearance during the first three hours is depicted in more detail. Values are expressed as mean ± SD of 14 patients, since pharmacokinetic data of patient #3 were incomplete.

Administration of ^{111}In-DOTA-girentuximab-IRDye800CW was well tolerated, as expected based on previous extensive experience with radiolabeled girentuximab [11, 12, 21, 22]. No prolongation of the QTc-interval was found and no study drug-related SAE were observed. In two patients (13%) hospital admission was prolonged due to complications of surgery (CTCAE grade III), which is in accordance with complication rates reported in the literature [23]. Thus, intraoperative dual-modality imaging with ^{111}In-DOTA-girentuximab-IRDye800CW is a safe procedure.

Considering the trend to treat larger and more complex tumors by NSS [8, 24, 25], there is an increasing need for tools to achieve complete tumor resection, while supporting oncologically safe NSS. The advantage of using NIR dyes over visible light dyes is that there is less autofluorescence, less scattering and a slightly higher tissue penetration depth [26]. Furthermore, since the dye is not visible by the human eye, the dye does not change the appearance of the surgical field, in contrast to, for example, blue dye. This implies that a light source and a camera system with special filters are needed, which can be argued as a disadvantage. NIRF after injection of indocyanine green has been used to delineate renal tumors. Indocyanine green accumulates in normal kidney parenchyma, resulting in relative hypofluorescence of RCC [27-29]. Disadvantages of this approach are that it is non-specific and hypofluorescent fat tissue can be misinterpreted as residual tumor tissue [27]. By targeting tumor-associated antigens, a positive T:N contrast can be obtained. Folate-receptor alpha-targeted NIRF has shown promise to detect superficial tumor lesions in ovarian cancer [1] and has also been explored in RCC, but conflicting results were reported [30, 31].

Because of the high expression of CAIX on more than 95% of primary ccRCC, CAIX is a more promising target for targeted imaging of ccRCC. The current study shows that CAIX-targeted dual-modality imaging could sensitively detect and delineate ccRCC during surgery. NIRF has the

additional advantage to assess the surgical margins *ex vivo* as well as the surgical cavity *in vivo*. The radiosignal allowed both preoperative evaluation of tumor extension with SPECT/CT and intraoperative tumor localization by gamma probe detection. The latter proved to be essential when perinephric fat covered the tumor and in largely endophytic tumors. An additional advantage of the radiolabel is that it allows accurate quantification (T:N ratio or %ID/g) of tracer accumulation, which is important as quantification of a fluorescence signal may be complicated due to scattering and attenuation of light in biological tissue. The main advantage of the dual-labeled approach over co-injection of two separate antibodies is that both signals originate from the same molecule. This may be important, as conjugating the antibody with fluorescent dyes may alter the in vivo behavior of the conjugate [15]. Previous analyses showed that radiolabeled girentuximab remained intact and could be visualized on tumor cells ex vivo [32-34]. Based on the ratios used, approximately 74% of the girentuximab molecules are truly dual-labeled (containing at least one DOTA and one IRDye800CW molecule) [15]. Thus, we assume that the quantification of the radiolabel is representative for targeting of the intact antibody. Indeed, we observed a perfect visual overlap between the fluorescence and radioactive image in ex vivo analysis (Fig. 4), substantiating that the antibody remained intact in the tumor. The very low accumulation of ^{111}In-DOTA-girentuximab-IRDye800CW in CAIX-negative tumors is adding to the evidence that uptake is primarily mediated by CAIX expression and only slightly by the enhanced permeability and retention effect. Therefore, preoperative ^{111}In-DOTA-girentuximab-IRDye800CW SPECT/CT imaging also has great diagnostic value since it allows for noninvasive confirmation that the tumor is a CAIX-expressing ccRCC. PET and SPECT studies with Iodine-124 labeled and Indium-111 labeled girentuximab, respectively, have shown the feasibility of this approach [11, 12, 21]. Distinction of ccRCC from other renal lesions can be difficult, since studies have shown that in up to 25% of patients that undergo surgery for small renal masses, final histology shows benign disease [35].

Despite the heterogeneous uptake of ^{111}In-DOTA-girentuximab-IRDye800CW in the tumor, a high T:N fluorescence contrast was observed at the tumor margins, which is essential for detection of tumor remnants and to subsequently guide additional resection of tumorous tissue. Van Driel et al. have shown that a minimum of 1 mm^3 tumor tissue could be detected with the NIRF system that was used in the current study [36]. Recently, we have shown in an animal model that submillimeter micrometastases could be detected with dual-modality imaging with dual-labeled antibodies [37]. However, the detection of small lesions is dependent on several factors, such as tumor vascularization, antigen expression, background tissue signal and tumor location. The highest T:N gamma probe ratio (3.3±0.64) was found at the 10 mg dose level and a trend towards a lower T:N contrast at higher protein doses was seen. Although the highest absolute amount (in theory the highest signal intensity) of protein per gram of tumor tissue (% ID/g × protein dose) was found at the 30 mg dose level, this resulted in a slightly decreased T:N contrast (gamma probe). This is in accordance with results of the studies with ^{131}I-girentuximab and may be attributed to antigen saturation at higher protein doses [10, 38]. Therefore, a protein dose of 10 mg was considered to be the optimal dose when taking into account both imaging modalities.

Addition of fluorescent molecules to a radiolabeled antibody may affect its biodistribution and tumor-specific accumulation. Animal studies have shown that the addition of up to two fluorescent molecules per girentuximab molecule (substitution ratio) only slightly effects its biodistribution and specific tumor accumulation [15]. Since the substitution ratio in the current study was between 1.0 and 2.0, no decrease in specific tumor accumulation was expected and indeed tumor uptake was comparable to radiolabeled girentuximab [22]. In addition, pharmacokinetic analyses confirmed that blood clearance of ^{111}In-DOTA-girentuximab-IRDye-800CW is similar to that of ^{111}Indium-DTPA-girentuximab ($t_{1/2}\beta$ 73.5±17.0 h versus $t_{1/2}\alpha+\beta$ 58±18 h) [39]. The required interval between tracer injection and tumor targeting of approximately 7 days implies that the surgeon should decide well before surgery if intraoperative imaging will be needed. Pharmacokinetics are faster with smaller molecules, but small molecules may have the disadvantage of high physiological renal clearance, thereby obscuring ccRCC tumors [40]. Besides low normal kidney uptake, a further advantage of IgG molecules over antibody fragments and small molecules is the convenient chemistry of radiolabeling and fluorescence labeling, without significantly compromising the immunoreactivity or altering the pharmacokinetics [15]. Previous studies with radiolabeled girentuximab have shown that high tumor-to-normal tissue ratios were obtained 4 to 7 days after injection [12, 41]. In the current study, we aimed to show the feasibility of dual-modality imaging and we preferred to perform both SPECT and fluorescence imaging between 4 to 7 days after injection. The choice to perform SPECT/CT imaging 4

days after injection and fluorescence imaging 7 days after injection was mainly based on logistical reasons. Future studies may focus on optimizing this time interval for dual-labeled girentuximab.

In the current study, dual-modality imaging devices were not integrated in the standard set of surgical instruments and therefore switching between standard surgery and dual-modality image-guided surgery took additional time. After introducing the standard surgical instruments and opening the retroperitoneum, the laparoscopic gamma probe was used to localize the tumor. After exposure of the tumor, the fluorescence camera was introduced. Subsequently, surgery was continued with the standard surgical instruments. Therefore, dual-modality imaging could only be performed before resection and after terminating the critical period of kidney ischemia and haemostasis, making deep surgical margins less accessible for NIRF. Integration of imaging devices into the standard surgical instruments would increase the convenient use of dual-modality imaging. Except for its use during NSS, the specific accumulation of ^{111}In-DOTA-girentuximab-IRDye800CW in ccRCC implies that dual-modality imaging may also be advantageous for lymph node dissection or metastasectomy. Since this was a phase I first in man study with the objective to assess the safety and feasibility, the surgical strategy (radical or partial nephrectomy) could not be changed based on intraoperative imaging results alone. Whether targeted dual-modality imaging using ^{111}In-DOTA-girentuximab-IRDye800CW reduces PSM or ccRCC recurrences needs to be studied in subsequent prospective studies.

Abbreviations

CAIX: carbonic anhydrase IX; ccRCC: clear cell renal cell carcinoma; T:N ratio: tumor-to-normal kidney ratio; PSM: positive surgical margin; NSS: nephron-sparing surgery; QTc interval: corrected QT interval; (S)AE: (serious) adverse event; CTCAE: common terminology criteria for adverse events; ID: injected dose; %ID/g: percentage of the injected dose per gram; NIRF: near-infrared fluorescence imaging; cps: counts per second; LN: laparoscopic nephrectomy; OPN: open partial nephrectomy; RAL(P)N: robot-assisted laparoscopic (partial) nephrectomy.

Acknowledgments

The authors thank D. Lobeek for her help with the pharmacokinetic analysis and D.L. Bos and M. de Weijert for their technical assistance.

Supplementary Material

Supplementary figures and tables.
http://www.thno.org/v08p2161s1.pdf
Movie S1. http://www.thno.org/v08p2161s2.mp4
Movie S2. http://www.thno.org/v08p2161s3.mp4

Competing Interests

The authors have declared that no competing interest exists.

References

1. van Dam GM, Themelis G, Crane LM, Harlaar NJ, Pleijhuis RG, Kelder W, et al. Intraoperative tumor-specific fluorescence imaging in ovarian cancer by folate receptor-alpha targeting: first in-human results. Nat Med. 2011; 17: 1315-9.
2. Okusanya OT, DeJesus EM, Jiang JX, Judy RP, Venegas OG, Deshpande CG, et al. Intraoperative molecular imaging can identify lung adenocarcinomas during pulmonary resection. J Thorac Cardiovasc Surg. 2015; 150: 28-35 e1.
3. Rosenthal EL, Warram JM, de Boer E, Chung TK, Korb ML, Brandwein-Gensler M, et al. Safety and Tumor Specificity of Cetuximab-IRDye800 for Surgical Navigation in Head and Neck Cancer. Clin Cancer Res. 2015; 21: 3658-66.
4. Koch M, de Jong JS, Glatz J, Symvoulidis P, Lamberts LE, Adams AL, et al. Threshold Analysis and Biodistribution of Fluorescently Labeled Bevacizumab in Human Breast Cancer. Cancer Res. 2016; 77: 623-31.
5. Lamberts LE, Koch M, de Jong JS, Adams ALL, Glatz J, Kranendonk MEG, et al. Tumor-Specific Uptake of Fluorescent Bevacizumab-IRDye800CW Microdosing in Patients with Primary Breast Cancer: A Phase I Feasibility Study. Clin Cancer Res. 2017; 23: 2730-41.
6. Ferlay J, Steliarova-Foucher E, Lortet-Tieulent J, Rosso S, Coebergh JW, Comber H, et al. Cancer incidence and mortality patterns in Europe: estimates for 40 countries in 2012. Eur J Cancer. 2013; 49: 1374-403.
7. Meyer C, Hansen J, Becker A, Schmid M, Pradel L, Strini K, et al. The Adoption of Nephron-Sparing Surgery in Europe - A Trend Analysis in Two Referral Centers from Austria and Germany. Urol Int. 2016; 96: 330-6.
8. Derweesh IH, Autorino R, Bensalah K, Capitanio U. Partial Nephrectomy for Large or Complex Masses: Option or Obsolete? Eur Urol. 2017; 72: 76-7.
9. Marszalek M, Carini M, Chlosta P, Jeschke K, Kirkali Z, Knuchel R, et al. Positive surgical margins after nephron-sparing surgery. Eur Urol. 2012; 61: 757-63.
10. Steffens MG, Boerman OC, Oosterwijk-Wakka JC, Oosterhof GO, Witjes JA, Koenders EB, et al. Targeting of renal cell carcinoma with iodine-131-labeled chimeric monoclonal antibody G250. J Clin Oncol. 1997; 15: 1529-37.
11. Divgi CR, Uzzo RG, Gatsonis C, Bartz R, Treutner S, Yu JQ, et al. Positron emission tomography/computed tomography identification of clear cell renal cell carcinoma: results from the REDECT trial. J Clin Oncol. 2013; 31: 187-94.
12. Muselaers CH, Boerman OC, Oosterwijk E, Langenhuijsen JF, Oyen WJ, Mulders PF. Indium-111-labeled girentuximab immunoSPECT as a diagnostic tool in clear cell renal cell carcinoma. Eur Urol. 2013; 63: 1101-6.
13. Stillebroer AB, Boerman OC, Desar IM, Boers-Sonderen MJ, van Herpen CM, Langenhuijsen JF, et al. Phase 1 radioimmunotherapy study with lutetium 177-labeled anti-carbonic anhydrase IX monoclonal antibody girentuximab in patients with advanced renal cell carcinoma. Eur Urol. 2013; 64: 478-85.
14. Muselaers CH, Stillebroer AB, Rijpkema M, Franssen GM, Oosterwijk E, Mulders PF, et al. Optical Imaging of Renal Cell Carcinoma with Anti-Carbonic Anhydrase IX Monoclonal Antibody Girentuximab. J Nucl Med. 2014; 55: 1035-40.
15. Rijpkema M, Bos DL, Cornelissen AS, Franssen GM, Goldenberg DM, Oyen WJ, et al. Optimization of dual-labeled antibodies for targeted intraoperative imaging of tumors. Mol Imaging. 2015; 14: 15-25.
16. Muselaers CH, Rijpkema M, Bos DL, Langenhuijsen JF, Oyen WJ, Mulders PF, et al. Radionuclide and fluorescence imaging of clear cell renal cell carcinoma using dual labeled anti-carbonic anhydrase IX antibody G250. J Urol. 2015; 194: 532-8.
17. Hekman MC, Boerman OC, de Weijert M, Bos DL, Oosterwijk E, Langenhuijsen JF, et al. Targeted Dual-Modality Imaging in Renal Cell Carcinoma: An Ex Vivo Kidney Perfusion Study. Clin Cancer Res. 2016; 22: 4634-42.
18. Tummers WS, Warram JM, Tipirneni KE, Fengler J, Jacobs P, Shankar L, et al. Regulatory Aspects of Optical Methods and Exogenous Targets for Cancer Detection. Cancer Res. 2017; 77: 2197-206.
19. Zinn KR, Korb M, Samuel S, Warram JM, Dion D, Killingsworth C, et al. IND-Directed Safety and Biodistribution Study of Intravenously Injected Cetuximab-IRDye800 in Cynomolgus Macaques. Mol Imaging Biol. 2015; 17: 49-57.
20. Lindmo T, Boven E, Cuttitta F, Fedorko J, Bunn PA, Jr. Determination of the immunoreactive fraction of radiolabeled monoclonal antibodies by linear

extrapolation to binding at infinite antigen excess. J Immunol Methods. 1984; 72: 77-89.
21. Divgi CR, Pandit-Taskar N, Jungbluth AA, Reuter VE, Gonen M, Ruan S, et al. Preoperative characterisation of clear-cell renal carcinoma using iodine-124-labelled antibody chimeric G250 (124I-cG250) and PET in patients with renal masses: a phase I trial. Lancet Oncol. 2007; 8: 304-10.
22. Steffens MG, Oosterwijk E, Zegwaart-Hagemeier NE, van't Hof MA, Debruyne FM, Corstens FH, et al. Immunohistochemical analysis of intratumoral heterogeneity of [131I]cG250 antibody uptake in primary renal cell carcinomas. Br J Cancer. 1998; 78: 1208-13.
23. Maurice MJ, Ramirez D, Kara O, Malkoc E, Nelson RJ, Fareed K, et al. Optimal outcome achievement in partial nephrectomy for T1 renal masses: A contemporary analysis of open and robotic cases. BJU Int. 2017; 120: 537-43.
24. Pavan N, Derweesh IH, Mir CM, Novara G, Hampton LJ, Ferro M, et al. Outcomes of Laparoscopic and Robotic Partial Nephrectomy for Large (>4 Cm) Kidney Tumors: Systematic Review and Meta-Analysis. Ann Surg Oncol. 2017; 24: 2420-8.
25. Mir MC, Derweesh I, Porpiglia F, Zargar H, Mottrie A, Autorino R. Partial Nephrectomy Versus Radical Nephrectomy for Clinical T1b and T2 Renal Tumors: A Systematic Review and Meta-analysis of Comparative Studies. Eur Urol. 2017; 71: 606-17.
26. Frangioni JV. In vivo near-infrared fluorescence imaging. Curr Opin Chem Biol. 2003; 7: 626-34.
27. Mitsui Y, Shiina H, Arichi N, Hiraoka T, Inoue S, Sumura M, et al. Indocyanine green (ICG)-based fluorescence navigation system for discrimination of kidney cancer from normal parenchyma: application during partial nephrectomy. Int Urol Nephrol. 2012; 44: 753-9.
28. Tobis S, Knopf JK, Silvers C, Messing E, Yao J, Rashid H, et al. Robot-assisted and laparoscopic partial nephrectomy with near infrared fluorescence imaging. J Endourol. 2012; 26: 797-802.
29. Tobis S, Knopf JK, Silvers CR, Marshall J, Cardin A, Wood RW, et al. Near infrared fluorescence imaging after intravenous indocyanine green: initial clinical experience with open partial nephrectomy for renal cortical tumors. Urology. 2012; 79: 958-64.
30. Shum CF, Bahler CD, Low PS, Ratliff TL, Kheyfets SV, Natarajan JP, et al. Novel Use of Folate-Targeted Intraoperative Fluorescence, OTL38, in Robot-Assisted Laparoscopic Partial Nephrectomy: Report of the First Three Cases. J Endourol Case Rep. 2016; 2: 189-97.
31. Guzzo TJ, Jiang J, Keating J, DeJesus E, Judy R, Nie S, et al. Intraoperative Molecular Diagnostic Imaging Can Identify Renal Cell Carcinoma. J Urol. 2016; 195: 748-55.
32. Oosterwijk-Wakka JC, de Weijert MC, Franssen GM, Leenders WP, van der Laak JA, Boerman OC, et al. Successful combination of sunitinib and girentuximab in two renal cell carcinoma animal models: a rationale for combination treatment of patients with advanced RCC. Neoplasia. 2015; 17: 215-24.
33. Steffens MG, Kranenborg MH, Boerman OC, Zegwaart-Hagemeier NE, Debruyne FM, Corstens FH, et al. Tumor retention of 186Re-MAG3, 111In-DTPA and 125I labeled monoclonal antibody G250 in nude mice with renal cell carcinoma xenografts. Cancer Biother Radiopharm. 1998; 13: 133-9.
34. Cheal SM, Punzalan B, Doran MG, Evans MJ, Osborne JR, Lewis JS, et al. Pairwise comparison of 89Zr- and 124I-labeled cG250 based on positron emission tomography imaging and nonlinear immunokinetic modeling: in vivo carbonic anhydrase IX receptor binding and internalization in mouse xenografts of clear-cell renal cell carcinoma. Eur J Nucl Med Mol Imaging. 2014; 41: 985-94.
35. Schachter LR, Cookson MS, Chang SS, Smith JA, Jr., Dietrich MS, Jayaram G, et al. Second prize: frequency of benign renal cortical tumors and histologic subtypes based on size in a contemporary series: what to tell our patients. J Endourol. 2007; 21: 819-23.
36. van Driel PB, van de Giessen M, Boonstra MC, Snoeks TJ, Keereweer S, Oliveira S, et al. Characterization and evaluation of the artemis camera for fluorescence-guided cancer surgery. Mol Imaging Biol. 2015; 17: 413-23.
37. Hekman MCH, Rijpkema M, Bos DL, Oosterwijk E, Goldenberg DM, Mulders PFA, et al. Detection of Micrometastases Using SPECT/Fluorescence Dual-Modality Imaging in a CEA-Expressing Tumor Model. J Nucl Med. 2017; 58: 706-10.
38. Steffens MG, Oosterwijk-Wakka JC, Zegwaart-Hagemeier NE, Boerman OC, Debruyne FM, Corstens FH, et al. Immunohistochemical analysis of tumor antigen saturation following injection of monoclonal antibody G250. Anticancer Res. 1999; 19: 1197-200.
39. Brouwers AH, Buijs WC, Oosterwijk E, Boerman OC, Mala C, De Mulder PH, et al. Targeting of metastatic renal cell carcinoma with the chimeric monoclonal antibody G250 labeled with (131)I or (111)In: an intrapatient comparison. Clin Cancer Res. 2003; 9: 3953S-60S.
40. Turkbey B, Lindenberg ML, Adler S, Kurdziel KA, McKinney YL, Weaver J, et al. PET/CT imaging of renal cell carcinoma with (18)F-VM4-037: a phase II pilot study. Abdom Radiol (NY). 2016; 41: 109-18.
41. Stillebroer AB, Zegers CM, Boerman OC, Oosterwijk E, Mulders PF, O'Donoghue JA, et al. Dosimetric analysis of 177Lu-cG250 radioimmunotherapy in renal cell carcinoma patients: correlation with myelotoxicity and pretherapeutic absorbed dose predictions based on 111In-cG250 imaging. J Nucl Med. 2012; 53: 82-9.